The Role of TLR4 Activation in Photoreceptor Mitochondrial Oxidative Stress

MinHee K. Ko, Sindhu Saraswathy, Jignesh G. Parikh, and Narsing A. Rao

Purpose. Herein the authors investigated whether the activation of Toll-like receptors (TLRs) in the innate immune response causes retinal photoreceptor oxidative stress and mitochondrial DNA (mtDNA) damage.

Methods. On day 5 after injection of complete Freund's adjuvant containing heat-killed *Mycobacterium tuberculosis* (CFA), retinas were submitted to polymerase chain reaction (PCR) array focused on the TLR signaling, or apoptosis, pathway. CFA-mediated TLR4 activation, oxidative stress, and mtDNA damage were determined in B10.RIII and knockout (KO) mice (recombination activation gene [*Rag*] 1^{KO}, $TLR4^{KO}$, myeloid differentiation primary response gene 88 [*MyD88*]^{KO}, tumor necrosis factor [*TNF*]-α^{KO}, or caspase 7^{KO} mice) using quantitative real-time PCR, enzyme-linked immunosorbent assay, Western blot analysis, and immunohistochemistry. The mycobacterial DNA load on the retina, brain, liver, and spleen was determined by real-time PCR after intracardiac perfusion.

Results. PCR array demonstrated the upregulation of TLRs and their signaling molecules in retinas of CFA-injected mice compared with those of control animals without inflammatory cell infiltration in the retina and uvea. Mycobacterial DNA was detected in the retinas of CFA-injected mice. Retinas of CFA-injected animals showed oxidative stress and mtDNA damage, primarily in the photoreceptor inner segments. Upregulated TLR4 was localized with $CD11b^{+}MHCII^{+}$ cells but not with $GFAP^{+}$ astrocytes. This oxidative stress/damage was similar in CFA-injected $Rag1^{KO}$ mice compared with wild-type controls. Such damage was absent in the retinas of CFA-injected $TLR4^{KO}$, $MyD88^{KO}$, and TNF-α^{KO} mice. CFA-mediated inducible nitric oxide synthase expression in the retina was significantly decreased in TNF-α^{KO} mice.

Conclusions. Retinal photoreceptors are susceptible to mitochondrial oxidative stress/mtDNA damage in robust TLR4-mediated innate immune response. (*Invest Ophthalmol Vis Sci.* 2011;52:5824–5835) DOI:10.1167/iovs.10-6357

Research on Toll-like receptors (TLRs), their activation, and signal transduction in cytokine generation has enhanced our understanding of the molecular events that lead to innate immune response, autoimmune disorder, and tissue damage.[1–4] Although diverse tissues can express TLRs, these receptors are mostly expressed on those immune cells that are likely to first encounter microbes.[5] On recognition of the molecular patterns of pathogens such as lipopolysaccharide (LPS), peptidoglycan, polyinosinic/polycytidylic acid, double-stranded RNA, and CpG DNA of microbes,[2,5,6] the TLR initiates a complex signaling cascade through several adaptor molecules, including the common adaptor protein myeloid differentiation factor (*MyD*) 88, protein kinase, and other signaling intermediates.[7–9] This signaling cascade causes activation of nuclear factor (*NF*)-κB, resulting in subsequent activation of the genes encoding proinflammatory cytokines such as tumor necrosis factor (*TNF*)-α, interleukin (*IL*)-1β, IL-6, IL-8, and IL-12 and of chemokines.[10] Although cytokine generation is crucial for host defense, it can also lead to tissue damage. Among these cytokines, TNF-α in particular causes tissue damage by generating reactive oxygen species (ROS).[11] Various studies implicate TLR activation in many diseases, including atherosclerosis, asthma, rheumatoid arthritis, demyelinating nervous diseases, ischemia/reperfusion injury to the heart, kidney, liver, and lung, and age-related macular degeneration.[12–20] However, there is no clear understanding of the molecular mechanism by which activation of TLR initiates the disease process.

Mycobacteria mixed with incomplete Freund's adjuvant (IFA) has been used to induce innate immune response, and adding a tissue-specific antigen to such a mixture is known to induce autoimmune organ-specific inflammation, such as experimental autoimmune uveitis (EAU) and experimental autoimmune encephalomyelitis.[21] However, destructive adjuvant arthritis can occur within 10 days after the administration of complete Freund's adjuvant (CFA) alone.[21–23] Recent studies suggest that TLR activation may play a role in the development of macular degeneration.[20] Systemic administration of heat-killed *Mycobacterium tuberculosis* is a well-recognized agent for the induction of the robust innate immune response, including TLR.[24,25]

Activation of TLR4 may lead to mitochondrial oxidative stress in central nervous system neurons and in hepatocytes.[13,26] Oxidative stress is implicated as an initial event leading to retinal damage in the pathogenesis of various retinal degenerations.[27,28] Mitochondrial oxidative damage may be the initial event leading to retinal degeneration for several reasons: first, mtDNA lacks histones; second, mtDNA is highly susceptible and vulnerable to oxidative damage caused by ROS generated from TNF-α/inducible nitric oxide synthase (iNOS); and third, if the damage is not repaired, it can lead to mitochondrial dysfunction and cell death caused by the release of cytochrome *c*, activation of caspases, and apoptosis.[29,30] We recently demonstrated photoreceptor mitochondrial oxidative stress and selective mitochondrial DNA damage in the early phase (days 4–7) of EAU, before inflammatory cell infiltration in the retina and uvea.[31,32] Such oxidative damage in the mitochondria may be the initial event leading to retinal degeneration in EAU. Moreover, the retinas of these animals showed the generation of proinflammatory cytokines at this early stage,

From the Doheny Eye Institute, Department of Ophthalmology, Keck School of Medicine, University of Southern California, Los Angeles, California.

Supported in part by National Eye Institute Grants RO1 EY019506, EY017347, and EY03040 and by an unrestricted grant from Research to Prevent Blindness.

Submitted for publication August 6, 2010; revised January 25 and April 19, 2011; accepted May 23, 2011.

Disclosure: **M.K. Ko**, None; **S. Saraswathy**, None; **J.G. Parikh**, None; **N.A. Rao**, None

Corresponding author: Narsing A. Rao, Doheny Eye Institute, Department of Ophthalmology, Keck School of Medicine, University of Southern California, 1450 San Pablo Street, DVRC 211, Los Angeles, CA 90033; nrao@usc.edu.

suggesting that cytokine generation could be due to TLR expression in response to subcutaneous injection of the mycobacterial agent. The current model of CFA-induced TLR activation in vivo is used to address initial events involved in the development of uveitis and the potential retinal damage from robust innate immune response.

The goal of this study was to determine, using a robust TLR activation model with systemic CFA administration, whether TLR activation in innate immune response causes oxidative stress and mtDNA damage in photoreceptors. We will elucidate the regulation of TLR and the TLR-mediated proinflammatory mediator and its role in oxidative mtDNA damage in the retina.

Materials and Methods

Animal Model

Animal care and use were in compliance with institutional guidelines and with the ARVO Statement for the Use of Animals in Ophthalmic and Vision Research. B10.RIII mice and knockouts (KO) of recombination activating gene (*Rag*) 1, TLR4, MyD88, TNF-α, caspase 7, and their wild-type (WT, C57BL/ScSn, or C57BL/6J) were purchased from Jackson Laboratory (Bar Harbor, ME). CFA containing 2.5 mg/mL heat-killed *M. tuberculosis* (strain H37Ra; Difco, Detroit, MI) was emulsified 1:1 vol/vol with saline solution. A total of 300 μL emulsion was injected subcutaneously in each of three sites: the base of the tail and both thighs, as described earlier.[33] The control groups were injected with IFA, which lacks mycobacterial components. At day 5 postinjection (D5 p.i.), the retina, brain, liver, and spleen were collected for polymerase chain reaction (PCR) array, real-time PCR, or Western blot analysis.

Pathway-Specific PCR Array

Retinas from five groups of B10.RIII mice were collected on D5 p.i.: CFA only, CFA + interphotoreceptor retinoid-binding protein (IRBP, retina antigen), IFA only, heat-killed *M. tuberculosis* (H37Ra, 3 mg/mL) only, and noninjected group. Each group included five mice, and their retinas were pooled as one sample before total RNA isolation. In particular, the CFA- and IFA-injected groups had biological triplicates for the mouse PCR array (RT^2 Profiler; SABioscience, Frederick, MD). These retinas were submitted for the mouse PCR arrays (RT^2 Profiler; SABioscience) focused on the TLR signaling and apoptosis pathway, which profiles the expression of 168 key genes involved in TLR-mediated signal transduction, innate immunity, and cell death pathway. The threshold cycle (Ct) difference (mean of three independent experiments) between the experimental and control groups was calculated and normalized to housekeeping genes, and the increase (*x*-fold) in mRNA expression was determined by the $2^{-\Delta\Delta Ct}$ method.[34]

PCR to Detect *M. tuberculosis*

After extensive intracardiac perfusion with saline containing heparin (10 U/mL), 50 mg each of retina, brain, liver, spleen, and skin sites of CFA injection were collected from B10.RIII mice (D5 p.i.; $n = 10$ in each group) and were digested overnight using a DNA genomic minikit (Purelink; Invitrogen, Carlsbad, CA). Various tissues from five CFA-injected mice without perfusion and five IFA-injected mice were used as controls. Retinas were pooled as one sample per group, and brain, liver, and spleen were individually analyzed. Quantitative real-time PCR using SYBR Green was performed using the forward primer IS6 (5′-AGGCGAACCCTGCCCAG-3′) and the reverse primer IS7 (5′-GATCGCTGATCCGGCCA-3′) to amplify a 122-bp fragment of the IS6110 multicopy element (GenBank accession no. X52471).[35] The PCR mixture consisted of 300 nM primers, SYBR Green (Supermix; Bio-Rad, Hercules, CA), and DNA template. PCR conditions included one cycle of 50°C for 2 minutes and 95°C for 3 minutes; 45 cycles at 95°C for 30 seconds, 60°C for 30 seconds, and 70°C for 1 minute. After PCR, melting curve analysis was performed. Genomic DNA of *M. tuberculosis* with concentrations of 10 ng to 10 pg was used as standard. A bacterial genome load of 0.25 fg (single bacteria copy) was used to calculate the total bacterial genome load per 1 μg extracted DNA.

Long-Extension Quantitative PCR to Detect Retinal mtDNA Damage

Retinas were collected from CFA-injected and noninjected B10.RIII mice (D5 p.i.; $n = 6$ for each group). The procedures for isolation and quantification of genomic DNA and PCR have been previously described.[31,36,37] Total genomic DNA was isolated with a DNA kit (EasyDNA Kit; Invitrogen), according to the manufacturer's protocol. Genomic DNA concentration was determined with dye (PicoGreen; Invitrogen) in a DNA assay kit (Quanti-iT High Sensitivity; Invitrogen), and fluorescence was measured with a fluorometer (Qubit; Invitrogen). The dye (PicoGreen; Invitrogen) has very low fluorescence and exhibits >1000-fold fluorescence enhancement on binding to dsDNA at an excitation wavelength of 485 nm and an emission wavelength of 535 nm. Quantitative PCR (qPCR) was performed (GeneAmp PCR system 9700 with the GeneAmp XL PCR kit; Applied Biosystems, Foster City, CA). Reaction mixtures contained 15 ng genomic DNA template, 1 U/reaction rTthDNA polymerase XL, 20 pmol primers, 100 ng/μL bovine serum albumin, 200 μM dNTPs, and 1.3 mM $MgCl_2$. PCR was initiated by hot start (75°C for 2 minutes) before the addition of the rTth enzyme. For amplification of mtDNA, the PCR program included initial denaturation at 94°C for 1 minute, 18 cycles of 94°C for 15 seconds, 65°C for 12 minutes, and a final extension at 72°C for 10 minutes. A short mtDNA fragment (117-bp) was amplified with the same program, except that the extension temperature was 60°C. Primer sequences were used as follows: for the 10-kb mitochondrial genome, 5′-GCC AGC CTG ACC CAT AGC CAT CAT ATT AT-3′ and 5′-GAG AGA TTT TAT GGG TGT ATT GCG G-3′; to normalize for mitochondrial copy number, 117-bp mitochondrial fragment 5′-CCC AGC TAC TAC CAT CAT TCA AGT-3′ and 5′-GAT GGT TTG GGA GAT GAT TGG TTG ATG-3′. DNA lesion frequencies were calculated as

Table 1. Upregulation of Toll-like Receptors and Related Signaling Genes in the Retinas of Each Group Compared to Those of IFA-Injected Mice in PCR Array

Gene	Fold Increase (±SEM)		
	CFA*	CFA+IRBP†	Mtb‡
TNF-α	1.58 (±0.07)	1.68 (±0.07)	1.97 (±0.4)
TLR4	1.61 (±0.07)	1.44 (±0.004)	1.6 (±0.05)
C/EBP	1.62 (±0.11)	1.59 (±0.01)	1.49 (±0.05)
Ly86	1.63 (±0.07)	1.11 (±0.11)	1.19 (±0.03)
TLR2	1.64 (±0.13)	1.54 (±0.03)	1.75 (±0.01)
IL-1R1	1.67 (±0.10)	1.54 (±0.06)	1.49 (±0.02)
CD14	1.86 (±0.09)	1.62 (±0.03)	1.69 (±0.06)
IL-6 Ra	2.52 (±0.31)	1.9 (±0.12)	1.71 (±0.12)
IFN-γ	2.54 (±0.33)	1.66 (±0.05)	3.94 (±0.34)
Ptgs2	2.62 (±0.16)	1.56 (±0.08)	1.6 (±0.17)
CCL2/MCP1	2.74 (±0.21)	2.96 (±0.03)	2.28 (±0.71)
IL-1β	3.11 (±0.30)	3.15 (±0.06)	3.38 (±0.18)

Biological triplicates of each sample from CFA, CFA+IRBP, heat-killed *M. tuberculosis* itself (Mtb), and IFA (each sample contained 5–10 retinas from five mice; day 5 p.i.) were submitted for the PCR array focused on the Toll-like receptors (TLR) signaling pathway. Among 84 functional genes involved in TLR signaling pathways, the significantly upregulated genes (>1.5 of fold increase; $^*P < 0.05$) compared with those of IFA-injected B10.RIII mice are shown. There was no significant difference among groups: $\dagger P > 0.05$ for CFA vs. CFA + IRBP. $\ddagger P > 0.1$ for CFA vs. Mtb and for IFA vs. noninjected (not shown). *LY86*, lymphocyte antigen 86; *Ptgs2*, prostaglandin-endoperoxide synthase 2; *CCL2/MCP1*, chemokine ligand 2/monocyte chemotactic protein 1.

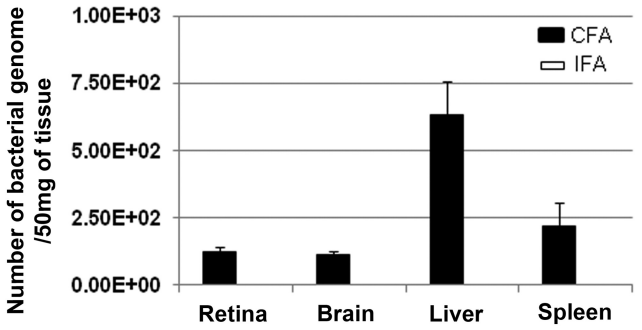

FIGURE 1. Detection of *M. tuberculosis* IS6110 multicopy element insertion sequence by quantitative real-time PCR analysis. Numbers of copies of *M. tuberculosis* in the retinas, brains, livers, and spleens of CFA-injected mice ($n = 10$) were quantified based on standard curve generated by standard *M. tuberculosis* genomic DNA. Note the presence of varying numbers of bacterial genome in the retinas, brains, livers, and spleens (50 mg each tissue). Tissues from IFA-injected B10.RIII mice ($n = 5$) were used as negative control for PCR. A bacterial genome load (0.25 fg for a single bacteria copy) was used to calculate the total bacterial genome load per 1 μg extracted DNA.

described previously.[29] Briefly, the fluorescence value of CFA-injected samples (A_D) was divided by those of untreated control (A_0), resulting in a relative amplification ratio. Assuming a random distribution of lesions and using the Poisson equation [$f(x) = e^{-\lambda}\lambda^x/x!$, where λ = the average lesion frequency] for the undamaged template (i.e., the zero class; $x = 0$), the average lesion frequency per DNA stand was determined as $\lambda = -\ln A_D/A_0$.[29] Statistical analysis was performed with a Student's *t*-test, and $P < 0.01$ was considered significant.

Immunohistochemistry for Localization of CFA-Mediated TLR4 Activation and mtDNA Damage

Eyes from CFA-injected B10.RIII, *MyD88*^{KO}, *Rag1*^{KO}, *TLR4*^{KO}, *TNF-α*^{KO}, and caspase 7^{KO} mice (D5 p.i.; $n = 6$–12 of each group) and their proper control mice were quickly embedded in compound (Tissue-Tek OCT; Sakura Finetek, Torrance, CA). Retinal cryosections (5–7 μm thickness) were fixed with 4% paraformaldehyde and further permeabilized/blocked in the blocking solution (5% bovine serum and 0.1% Triton X-100). Sections were incubated overnight at 4°C with combinations of the following primary antibodies (1:100 dilution) in the blocking solution: rat anti-mouse CD11b (Serotec, Raleigh, NC), rabbit anti-mouse TLR4 (Santa Cruz Biotechnology, Santa Cruz, CA), mouse anti-major histocompatibility complex (MHC) class II (Santa Cruz Biotechnology), goat anti-mouse glial fibrillary acidic protein (GFAP; Santa Cruz Biotechnology), rabbit anti-cytochrome *c* oxidase, subunit IV (Invitrogen), goat anti-8-hydroxy-deoxy-guanosine (8-OHdG; Millipore, Billerica, MA), mouse anti-TNF-α (Millipore), rabbit anti-TNFR1 (Stressgen, San Diego, CA), rabbit anti-iNOS/NOS type II (BD, San Jose, CA), and mouse anti-caspase 7 (Santa Cruz Biotechnology). The sections were further incubated for 1 hour at room temperature (RT) with secondary antibodies: Cy-3, Cy-5, and/or Cy-2-conjugated donkey anti-mouse, -rat, -goat and/or -rabbit antibody (1:200; Jackson ImmunoResearch Laboratories, West Grove, PA) and then were mounted using mounting medium containing DAPI (Vectashield; Vector Laboratories, Burlingame, CA). A negative control was processed using the same protocol with the omission of the primary antibody to assess nonspecific labeling and isotype control. Sections were analyzed with a confocal laser scanning microscope (510; Zeiss, Thornwood, NY).

The additional sections were stained with hematoxylin and eosin (H&E) and were examined by light microscopy for inflammatory cell infiltration and morphologic change.

Real-Time PCR to Confirm PCR Array

Total RNA from the retinas of CFA-injected B10.RIII mice and from controls (D5 p.i., $n = 12$ of each group) was prepared using reagent (TriZol; Invitrogen) for cDNA synthesis (Omniscript RT kit; Qiagen, Valencia, CA). One-fifth of the resultant cDNA was used for further PCR amplification. Each PCR reaction mixture contained a master mix (SYBR Green I; Bio-Rad) with 0.5 μM gene-specific primers: *TLR4*, 5′-AAG AAC ATA GAT CGA GCT TCA ACC C-3′ and 5′-GCT GTC CAA TAG GGA AGC TTC TAG AG-3′; *TNF-α*, 5′-CTA CTC CCA GGT TCT CTT CAA-3′ and 5′-GCA GAG AGG AGG TTG ACT TTC-3′; *iNOS*, 5′-CAG CTG GGC TGT ACA AAC CTT-3′ and 5′-CAT TGG AAG TGA AGC GTT TCG-3′; glyceraldehyde-3-phosphate dehydrogenase (*GAPDH*), 5′-CAC CAC CAT GGA GAA GGC-3′ and 5′-GCT AAG CAG

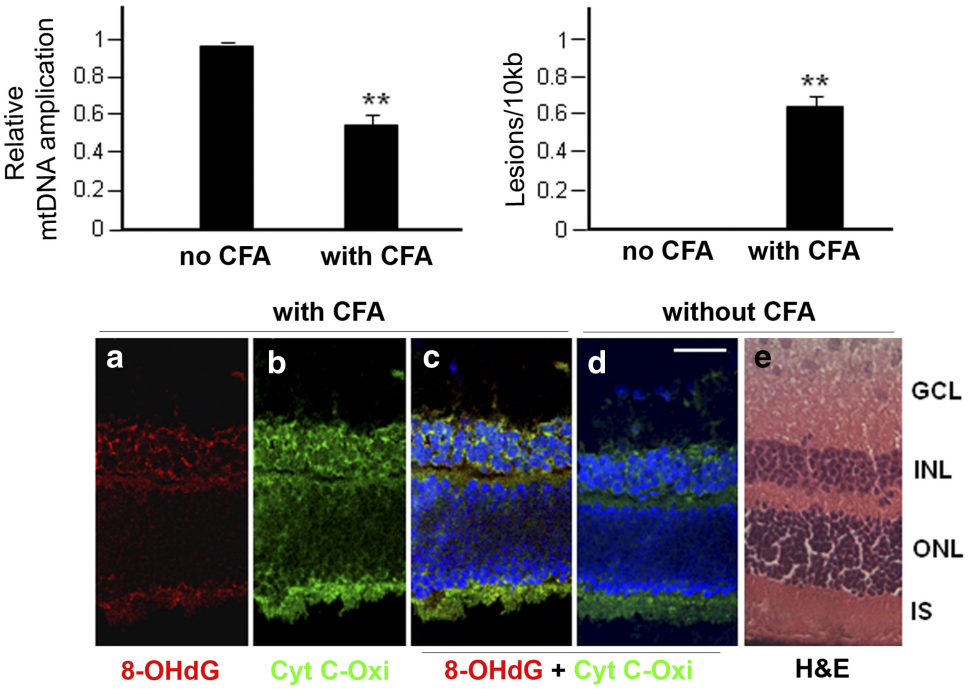

FIGURE 2. Increased mtDNA damage in the retinas of CFA-injected B10.RIII mice on day 5 p.i. (**A**) There was a significant decrease in mtDNA amplification in the retinas of CFA-injected group compared with those of the noninjected group. (**B**) The increased number of DNA lesions in retinas of CFA-injected mice. In retinas of CFA-injected mice, the frequency of mtDNA lesions was calculated to be 0.57 in 10 kb mitochondrial genome. All values represent three independent experiments. $^{**}P < 0.01$, $n = 5$ per each group. (**C**) 8-OHdG (**a**) oxidative DNA damage marker was colocalized with cytochrome *c* oxidase, subunit IV (Cyt C-Oxi, (**b**), which is localized in mitochondria in the IS and INL, (**c**) which was compared with those in the control (**d**). H&E-stained corresponding retinal section (**e**). ONL: outer nuclear layer. Scale bar, 50 μm.

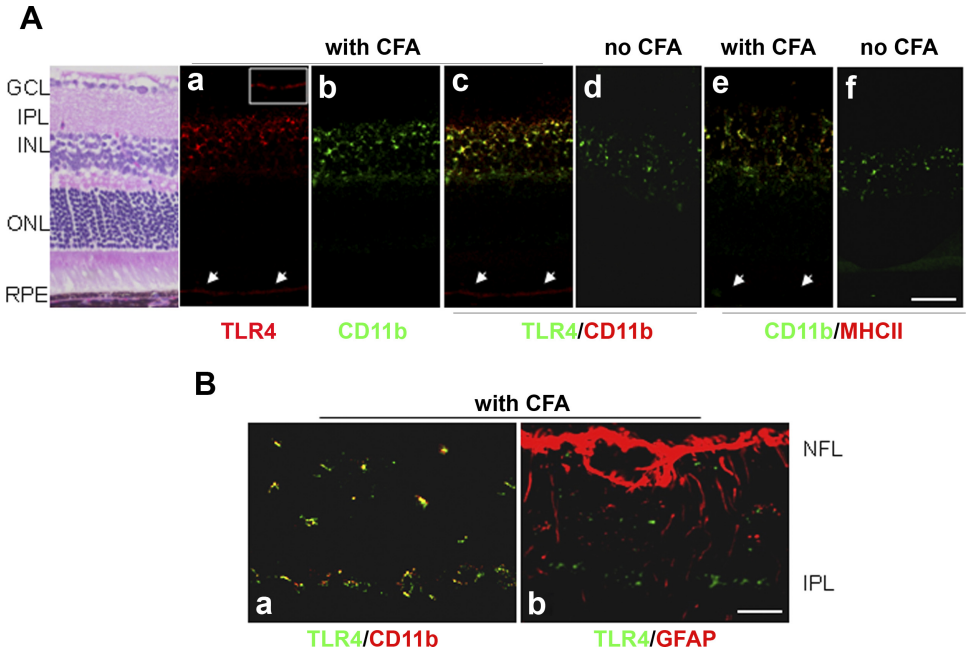

Figure 3. Localization of TLR4 expression in the retinas of CFA-injected B10.RIII mice. (**A**) TLR4$^+$ (**a**, *red*) and CD11b$^+$ microglia (**b**, *green*) showed colocalization (**c**, *yellow*) primarily in the IPL and INL in retinas of CFA-injected mice compared with those of the noninjected control (**d**). CD11b$^+$ microglia were colocalized with MHCII$^+$ cells in IPL and INL (**e**) in the retinas of CFA-injected mice compared with those of the noninjected control (**f**). Retinal pigment epithelium (RPE, *arrow*) of CFA-injected mice showed immunoactivity for TLR4 (**a**, *inset* of TLR4-positive immunoactivity on the RPE layer) but not for CD11b (**b**) and MHCII (**e**). Scale bar, 50 μm. (**B**) TLR4 expression was specifically localized on the CD11b$^+$ microglia in the retina (**a**, *yellow*) with CFA injection, whereas, GFAP$^+$ cells (**b**, *red*) (astrocytes, Muller cells, or both) did not show colocalization with TLR4 (**b**, *green*). Six to eight sections (40 μm apart) of each mouse (n = 10 per group) were analyzed for immunostaining. ONL, outer nuclear layer; NFL, nerve fiber layer. Scale bar, 20 μm.

TTG GTG GTG CA-3′. PCR amplification was performed using 40 cycles at 95°C for 30 seconds, 55°C to 60°C for 30 seconds, and 72°C for 1 minute, after a hot start at 95°C for 3 minutes in 25 μL reaction mixture (iCycler Optical System; Bio-Rad). PCR reactions for each gene were performed in triplicate on each cDNA template with the housekeeping gene *GAPDH*. The specificity of the amplicon was checked by performing dissociation melting curve analysis. The threshold cycle (Ct) difference (mean of three independent experiments) between the experimental and the control groups was calculated and normalized to GAPDH, and the increase (x-fold) in mRNA expression was determined by the $2^{-\Delta\Delta Ct}$ method.[34] Statistical analysis of ΔCt was performed with a Student's t-test for three independent samples, with significance set

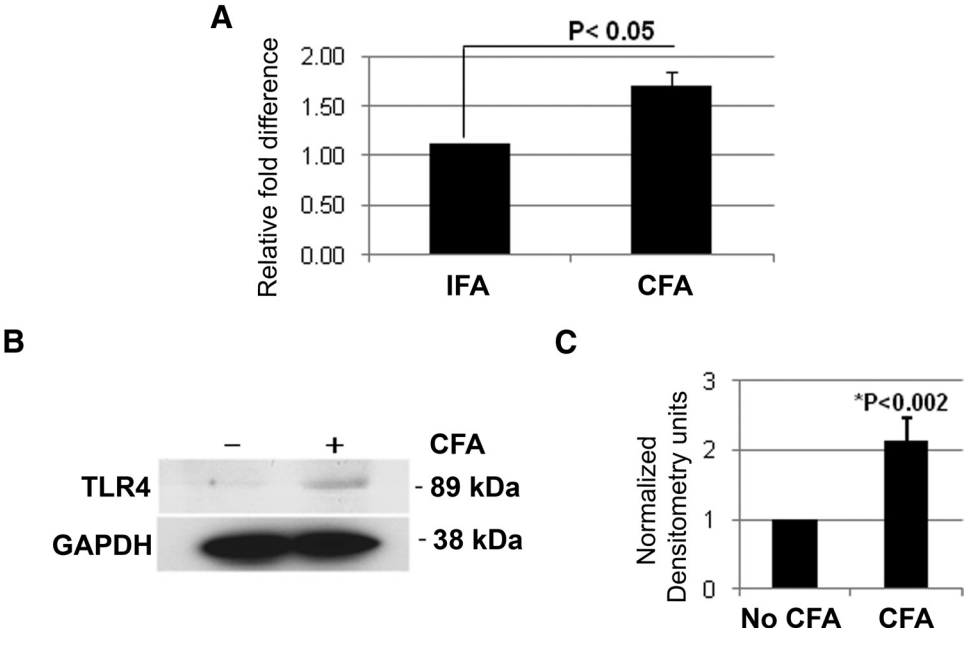

Figure 4. TLR4 expression in retinas of CFA-injected B10.RIII mice. (**A**) There was significant upregulation of TLR4 in retinas of CFA-injected mice compared with those of IFA-injected mice (n = 12 of each, biological triplicates) using real-time PCR. (**B**) TLR4 was upregulated in retinas of CFA-injected mice compared with those of control mice using Western blot analysis on retinal cell lysates (40 μg each group, n = 12). Rabbit anti-TLR4 or mouse anti-GAPDH (glyceraldehyde-3-phosphate dehydrogenase) as a primary antibody was used. (**C**) TLR4 bands from biological triplicates were quantified, and the densitometry showed significant upregulation of TLR4 in retinas of CFA-injected mice.

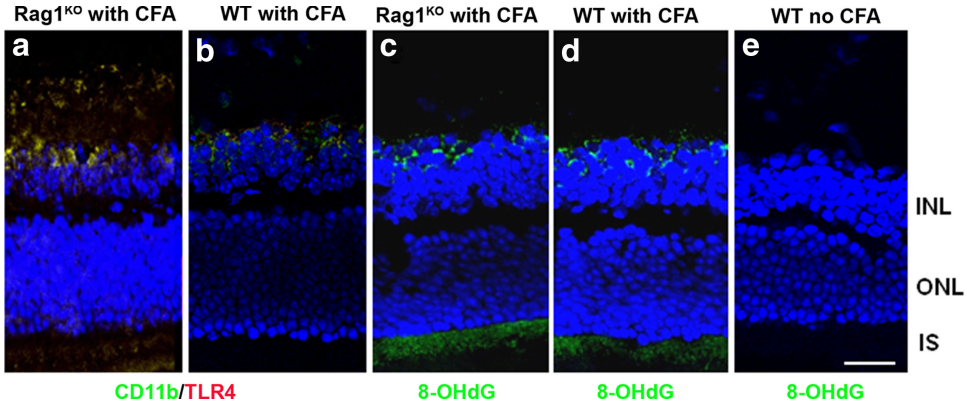

Figure 5. CFA-mediated TLR4 expression and mtDNA damage in *Rag1*^{KO} mice. TLR4 was colocalized with CD11b^{+} microglia in the retinas of CFA-injected *Rag1*^{KO} mice (**a**), which showed similar staining in the retinas of CFA-injected WT mice (**b**). 8-OHdG staining was seen in the IS of the photoreceptors and INL in the *Rag1*^{KO} mice similar to staining in CFA-injected WT mice (**c**, **d**). Noninjected controls showed no staining of 8-OHdG (**e**). ONL, outer nuclear layer. Scale bar, 50 μm.

as $P < 0.05$, and compared between the CFA-injected and control groups.

Western Blot Analysis

Biological triplicates were used for Western blot analysis. For each independent experiment, retinas were pooled from each experimental group, and the control groups ($n = 4$–5 of each group) were homogenized in protein extraction buffer (M-PER; Thermo Scientific, Pittsburgh, PA) combined with 1× protease inhibitor cocktails (Calbiochem, San Diego, CA). The proteins were separated by 7.5% to 15% SDS-PAGE–reduced gel and transferred by wet transfer unit (Bio-Rad) to PVDF membrane (Bio-Rad). The membranes were blocked with 5% nonfat milk in 1× TTBS (20 mM Tris-HCl, pH 7.5, 500 mM NaCl, 0.1% [vol/vol] Tween-20) for 1 hour at RT then incubated with primary antibody in blocking solution for 1 hour at RT. The membranes were further incubated in secondary antibody

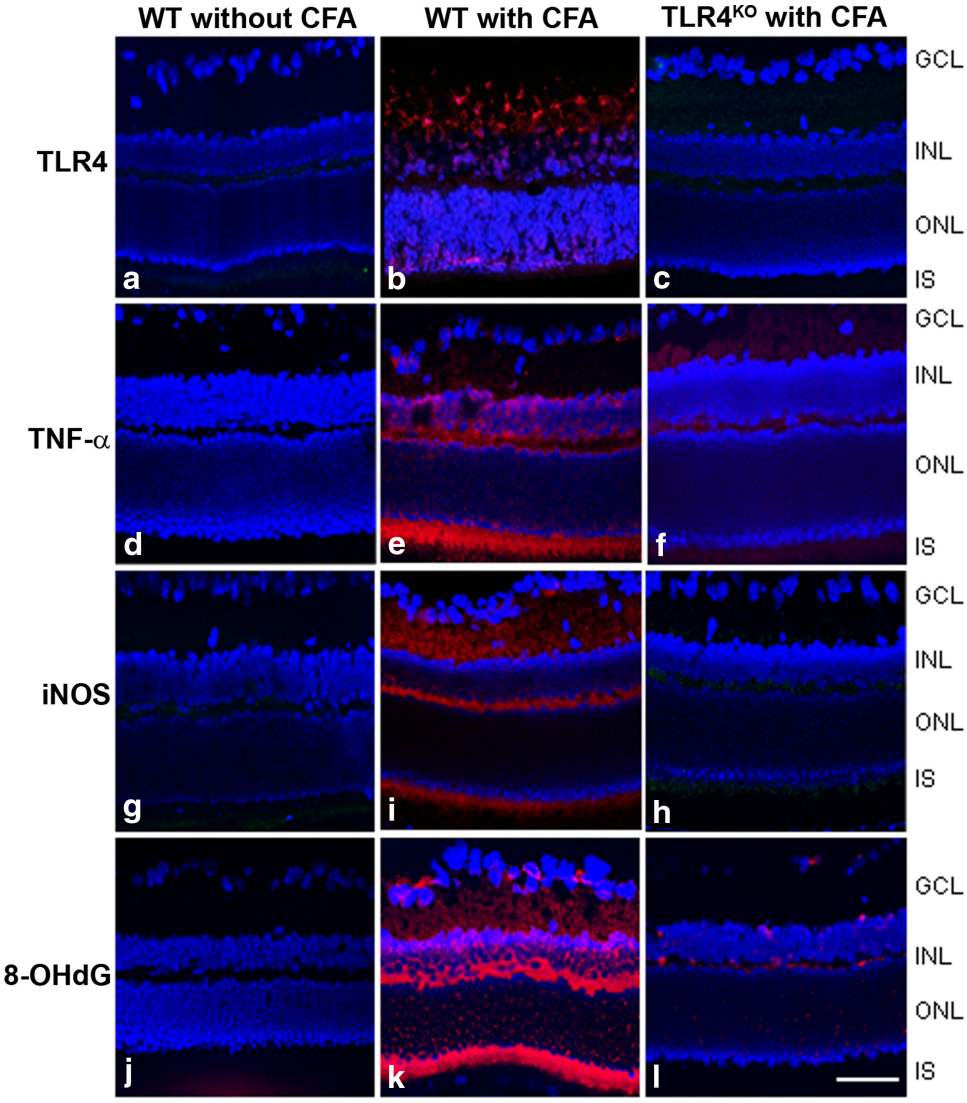

Figure 6. TNF-α, iNOS, and 8-OHdG expression in a TLR4-dependent manner. *TLR4*^{KO} and its WT control were injected with CFA, and retinas were collected on day 5 p.i. Randomized retinal sections (6–8 sections per eye) were immunostained with rabbit anti-TLR4 (**a**–**c**), mouse anti-TNF-α (**d**–**f**), mouse anti-iNOS (**g**, **h**), and goat anti-8-OHdG (**j**–**l**) primary antibodies, followed by Cy3-conjugated secondary antibodies. Immunoreactivity of TNF-α (**e** vs. **f**), iNOS (**i** vs. **h**), and 8-OHdG (**k** vs. **l**) in the retinas of CFA-injected *TLR4*^{KO} mice was reduced compared with those of CFA-injected WT, which were at a similar level shown in noninjected WT (**d**, **g**, **j**). ONL, outer nuclear layer. Scale bar, 50 μm.

after washing with 1× TTBS and then visualized (Luminol-ECL; GE Healthcare Bio-Sciences Corp, Piscataway, NJ). Rabbit anti-TLR4 (1:250 dilution; Santa Cruz Biotechnology), mouse anti-GAPDH (1:5000; Millipore), mouse anti-TNF-α (1:500; Santa Cruz Biotechnology), and rabbit anti-caspase 3 (1:250; Santa Cruz Biotechnology) were used as primary antibodies. Donkey anti-mouse and rabbit IgG-HRP conjugated antibody (1:2000; Santa Cruz Biotechnology) were used as secondary antibodies.

Quantitative Enzyme-Linked Immunosorbent Assay for TNF-α

Levels of proinflammatory cytokine TNF-α in mouse serum were analyzed using commercially available high-sensitivity enzyme-linked immunosorbent assay (ELISA) kits (Quantikine; R&D Systems, Minneapolis, MN), according to the manufacturer's instructions.

Statistical Analysis

Data are expressed as mean ± SEM for the indicated number of individual experiments. Student's *t*-test was used to analyze the results. $P < 0.05$ was considered statistically significant.

Results

CFA-Mediated Activation of Innate Immune Response Genes in Retinas

We determined CFA-mediated activation of the innate immune response in the retina using PCR array focused on the TLR signaling pathway. Among 84 functional TLR signaling genes, 12 were significantly upregulated (relative fold difference >1.5; $P < 0.05$; Table 1) in retinas of CFA-injected mice compared with those of IFA-injected mice. Moreover, there was no significant alteration of those genes in the CFA with IRBP or heat-killed *M. tuberculosis*–injected group compared with those of the CFA-injected group ($P > 0.1$). *TLR2* and *TLR4* as pattern recognition receptors were upregulated (~1.6-fold increase), and proinflammatory cytokines/chemokines, including chemokine ligand 2 (*CCL2*), *TNF-α*, interferon gamma (*IFN-γ*), *IL-1β*, *IL*-1R1, and *IL-6Ra*[38] were also upregulated (1.5- to 3.1-fold increase) in the retinas of CFA-injected mice. As molecules involved in the TLR4 signaling pathway, *CD14* (1.86-fold increase)[39] and lymphocyte activator 86 (1.63-fold increase; *LY86* known as myeloid differentiation 1)[40] were also upregulated in the retinas of CFA-injected B10.RIII. *C/EBP* (CCAAT/enhancer binding protein) showed an increase (1.62-fold increase) as a family of transcription factors interacting with *NF-κB* (1.26-fold increase; $P = 0.04$; not shown in Table 1) in addition to prostaglandin-endoperoxide synthase 2 (2.62-fold increase; known as cyclooxygenase 2) involved in inflammation.[41]

We further determined inflammatory cell infiltration. Randomly selected H&E-stained sections were examined, and no inflammatory cells were found in the retinas or uveae of the CFA-injected animals on D5 p.i. (data not shown).

Detection of *M. tuberculosis* in the Retina, Liver, and Spleen

To investigate whether bacterial products were mobilized to the retina from the distant injection site, we performed highly sensitive qPCR to determine the presence of bacterial DNA in the various tissues.[35] Aside from the subcutaneous depot at the injection site (80,142 copies in 50 mg tissue), the bacterial loads in the retina, brain, liver, and spleen ranged from 120 to 780 copies in 50 mg sample tissue (Fig. 1). No *M. tuberculosis* genome was detected from such tissue of IFA-injected mice. We found more of the *M. tuberculosis* genome, but the amount was not statistically significant in the tissues of nonperfused animals compared with those of perfused animals.

Mitochondrial DNA Damage in CFA-Injected B10.RIII Mice

We further determined whether upregulated innate immune response genes found in the PCR array (Table 1) were correlated with retinal mtDNA damage using a long-extension quantitative PCR-based method. Relative mtDNA amplification was decreased (Fig. 2A; ~50% reduction, $P < 0.01$) in retinas of CFA-injected mice compared with those of noninjected mice. The frequency of mtDNA lesions was higher in retinas of CFA-injected mice and was calculated to be 0.57 in 10 kb (Fig. 2B). Because each mtDNA is approximately 16 kb in length and each mitochondrion regularly contains 2 to 10 copies of mtDNA,[29] each mitochondrion contains approximately five lesions in the retinas of CFA-injected mice.

CFA-mediated DNA damage was further confirmed using oxidized DNA marker 8-OHdG immunostaining. In retinas of CFA-injected mice, 8-OHdG staining was seen in the inner nuclear layer (INL) and inner segment (IS) of photoreceptors, as well as in the ganglion cell layer (GCL; Fig. 2Ca), which colocalized with cytochrome *c* oxidase used as a mitochondria marker (Fig. 2Cb). Colocalization of 8-OHdG and cytochrome *c* oxidase (Fig. 2Cc, yellow) was absent in control animals (Fig. 2Cd). Moreover, 8-OHdG did not colocalize with nuclear staining (DAPI staining, blue; Fig. 2Cc), suggesting the presence of oxidative stress, specifically in the mitochondria.

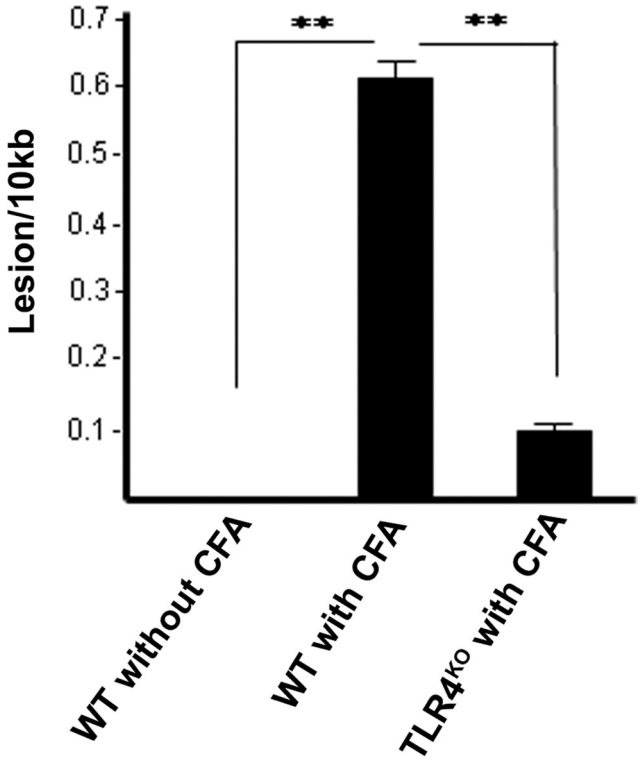

Figure 7. Decreased oxidative mtDNA damage in the retinas of CFA-injected *TLR4*^{KO} mice. The graph represents the number of DNA lesions per 10 kb mitochondrial genome, as determined by quantitative PCR. A significant number of DNA lesions in the retinas of CFA-injected WT were reduced in the retinas of CFA-injected *TLR4*^{KO} mice. All values represent biological triplicate. $^{**}P < 0.05$.

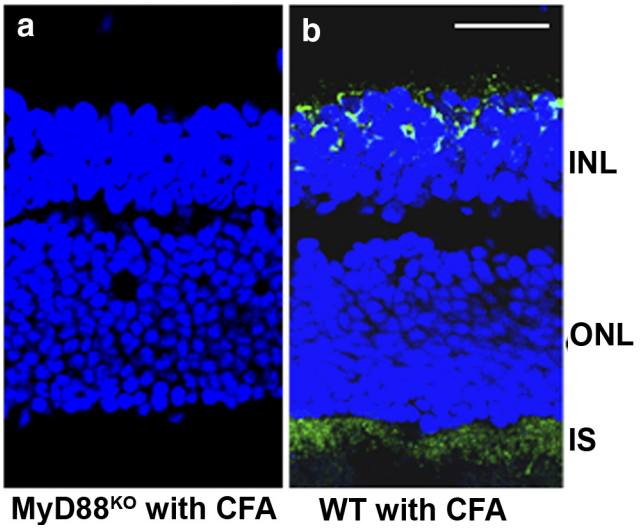

FIGURE 8. Absence of CFA-mediated oxidative stress in *MyD88*^{KO} mice. Absence of 8-OHdG immunostaining in the retinas of *MyD88*^{KO} mice injected with CFA (**a**), whereas CFA-injected WT showed 8-OHdG staining in the retina (**b**) in the IS and the INL. ONL, outer nuclear layer. Representative photograph is shown; six mice per group were used. Scale bar, 50 μm.

TLR4 Expression in the Retinas of CFA-Injected B10.RIII Mice

In PCR array, *CD14* and *LY86* related to the TLR4 signaling pathway were significantly upregulated along with *TLR4* in retinas of CFA-injected B10.RIII mice. We further studied the role of CFA-mediated TLR4 activation in the retina. Subcellular localization of TLR4 in the retina was determined using the markers of microglia (CD11b, F4.80, or Iba-1)[42] from CFA-injected and noninjected B10.RIII mice at D5 p.i. (Fig. 3). In the retinas of CFA-injected B10.RIII mice, immunoactivity of TLR4 (Fig. 3Aa) and CD11b (Fig. 3Ab) staining showed colocalization (Fig. 3Ac, yellow), mostly in the inner plexiform layer (IPL) and the INL, compared with those of noninjected control mice (Fig. 3Ad). Retinal pigment epithelium (RPE; Figs. 3Aa, 3Ac, arrow) of CFA-injected mice showed immunoactivity for TLR4 (Fig. 3Aa) but not for CD11b (Fig. 3Ab). CD11b$^+$ microglia in IPL and INL were colocalized with MHCII (Fig. 3Ae, yellow), which was upregulated in CFA-injected mice compared with noninjected mice (Fig. 3Af); however, staining of a minor part of TLR4 immunoactivity (Fig. 3Ac, red) was not completely coincident with that of CD11b. Other cell types may show TLR4-positive staining similar to the TLR4 staining in RPE, which shows TLR4$^+$CD11b$^-$MHCII$^-$ immunoactivity. TLR4 expression was specifically localized on the CD11b$^+$ microglia in the retina (Fig. 3Ba, yellow) with CFA injection, whereas GFAP$^+$ cells (Fig. 3Bb, red) (astrocytes and/or Muller cells) showed no colocalization with TLR4 (Fig. 3Bb, green). These data suggest that CD11b$^+$MHCII$^+$ microglia are the primary cells in CFA-mediated activation of the innate immune response.

Upregulation of TLR4 was further determined by real-time PCR and Western blot analysis, as shown in Figure 4. TLR4 was upregulated 1.71-fold ($P < 0.05$; Fig. 4A) and showed elevated TLR expression (Fig. 4B).

Oxidative DNA Damage in the Retina of Rag1^{KO} Mice with Innate Immune Response

We investigated whether adaptive immunity contributes to the induction of oxidative stress using *Rag1*^{KO} mice, which are deficient in T and B cells. These *Rag1*^{KO} mice have been

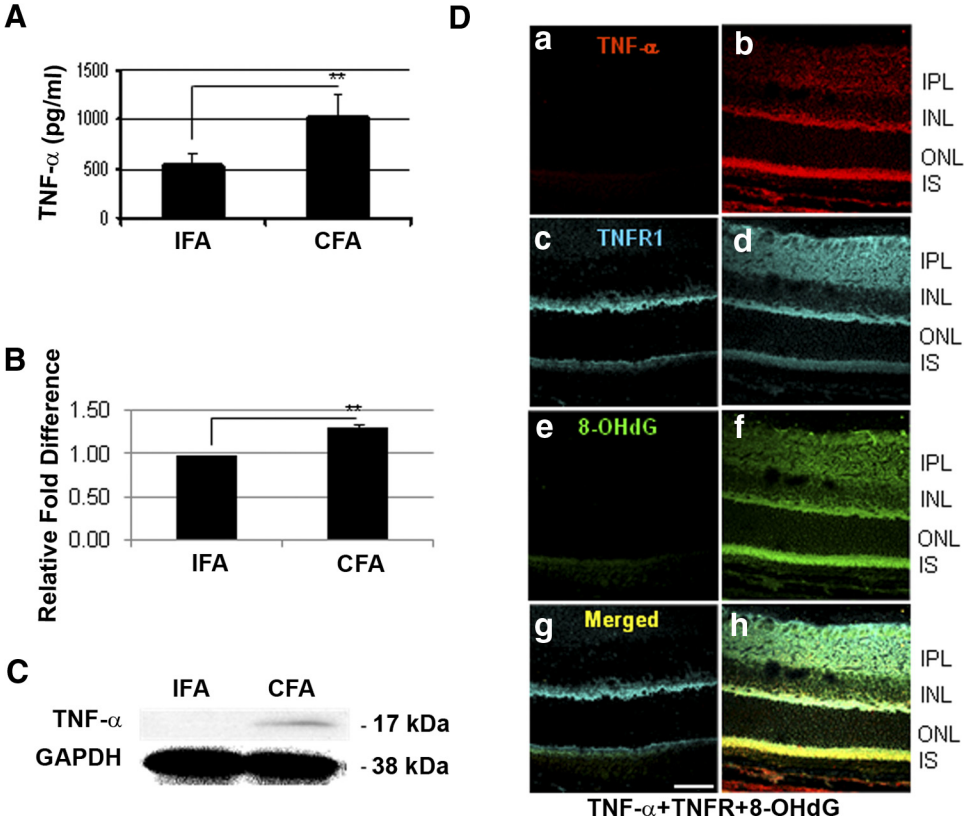

FIGURE 9. TNF-α expression in the retinas of B10.RIII mice injected with CFA. (**A**) TNF-α levels (pg/mL, $\pm$ SD) in the serum, measured by ELISA, were elevated in CFA-injected mice compared with IFA-injected B10.RIII mice (**$P = 0.02$; $n = 6$ per group). (**B**) Upregulation of TNF-α gene in retinas of CFA-injected B10.RIII mice ($n = 6$ of each group) compared with those of IFA-injected group in real-time RT-PCR. (**C**) TNF-α expression in retinas of CFA-injected compared with those of IFA-injected B10.RIII mice ($n = 12$ of each group) was analyzed by Western blot analysis. Cell lysates (40 μg) were separated by SDS-PAGE on 15% reduced gel. Mouse anti-TNF-α or GAPDH was used as a primary antibody, followed by HRP-conjugated anti-mouse antibody. Biological triplicates were performed. (**D**) Immunostaining of TNF-α, TNFR1, and 8-OHdG in the retina. There was no immunostaining of TNF-α in noninjected mice (**a**); however, TNF-α was localized in the IPL, INL, and IS of photoreceptors of the CFA-injected mice (**b**). CFA-mediated TNF-α expression was colocalized with TNFR1 (**c** vs. **d**) and 8-OHdG (**e** vs. **f**) in the IPL and IS of photoreceptors (**h** vs. **g**). Scale bar, 50 μm.

used extensively as a model with which to study the roles of innate and adaptive immunity.[43,44] TLR4 was colocalized on the CD11b$^+$ microglial cells (Fig. 5a) near the IPL and INL in the retinas of CFA-injected *Rag1*^{KO} mice; the staining was similar to the results seen in retinas of CFA-injected WT controls (Fig. 5b). 8-OHdG, the oxidized DNA damage marker, was detected and immunolocalized to the IS of the photoreceptors and the INL in retinas of CFA-injected *Rag1*^{KO} mice (Fig. 5c); staining was similar to that of CFA-injected WT controls (Fig. 5d). Localization of TLR4 on the CD11b$^+$ microglia and oxidative DNA damage in *Rag1*^{KO} indicates that the adaptive immune response does not play a role in the mtDNA damage of animals injected with CFA.

Role of TLR4 in Oxidative Stress and mtDNA Damage in Innate Immune Response

To further investigate the direct role of TLR4 in mtDNA damage in the retina, *TLR4*^{KO} (C57BL/10ScNJ) and WT mice (WT, C57BL/ScSn) were used. Compared with those of non-injected WT controls (Figs. 6a, 6d, 6g, 6j), there was a strong immunoreactivity of TLR4 (Fig. 6b vs. 6a), TNF-α (Fig. 6e vs. 6d), iNOS (Fig. 6i vs. 6g), and 8-OHdG (Fig. 6k vs. 6j) in the INL and IS of photoreceptors of the retinas of CFA-injected WT animals. In contrast, immunoactivity of TLR4 (Fig. 6c vs. 6b), TNF-α (Fig. 6f vs. 6e), iNOS (Fig. 6h vs. 6i), and 8-OHdG (Fig. 6l vs. 6k) was reduced in the retinas of CFA-injected *TLR4*^{KO} mice on D5 p.i. compared with those of CFA-injected WT mice.

We further detected a significant reduction in the mitochondrial DNA strand breaks in retinas of CFA-injected *TLR4*^{KO} mice compared with those of the CFA-injected WT mice (Fig. 7), supporting our previous observation that TLR4 activation plays an essential role in oxidative stress and DNA damage in innate immunity.

MyD88-Dependent Oxidative Stress in Innate Immune Response

TLR signals mostly through MyD88, which is a universal adapter protein of all TLR (except TLR 3) to activate the transcription factor NF-κB.[45] We further addressed the significance of MyD88 interaction with TLR and TLR4-mediated oxidative mtDNA damage. There was no immunoactivity of oxidized DNA marker 8-OHdG in the INL and photoreceptors (Fig. 8a) of retinas of CFA-injected *MyD88*^{KO} mice. In contrast, the retinas of CFA-injected WT mice showed strong positive 8-OHdG staining (Fig. 8b), suggesting that CFA-mediated oxidative stress and mtDNA damage in the retina is MyD88 dependent.

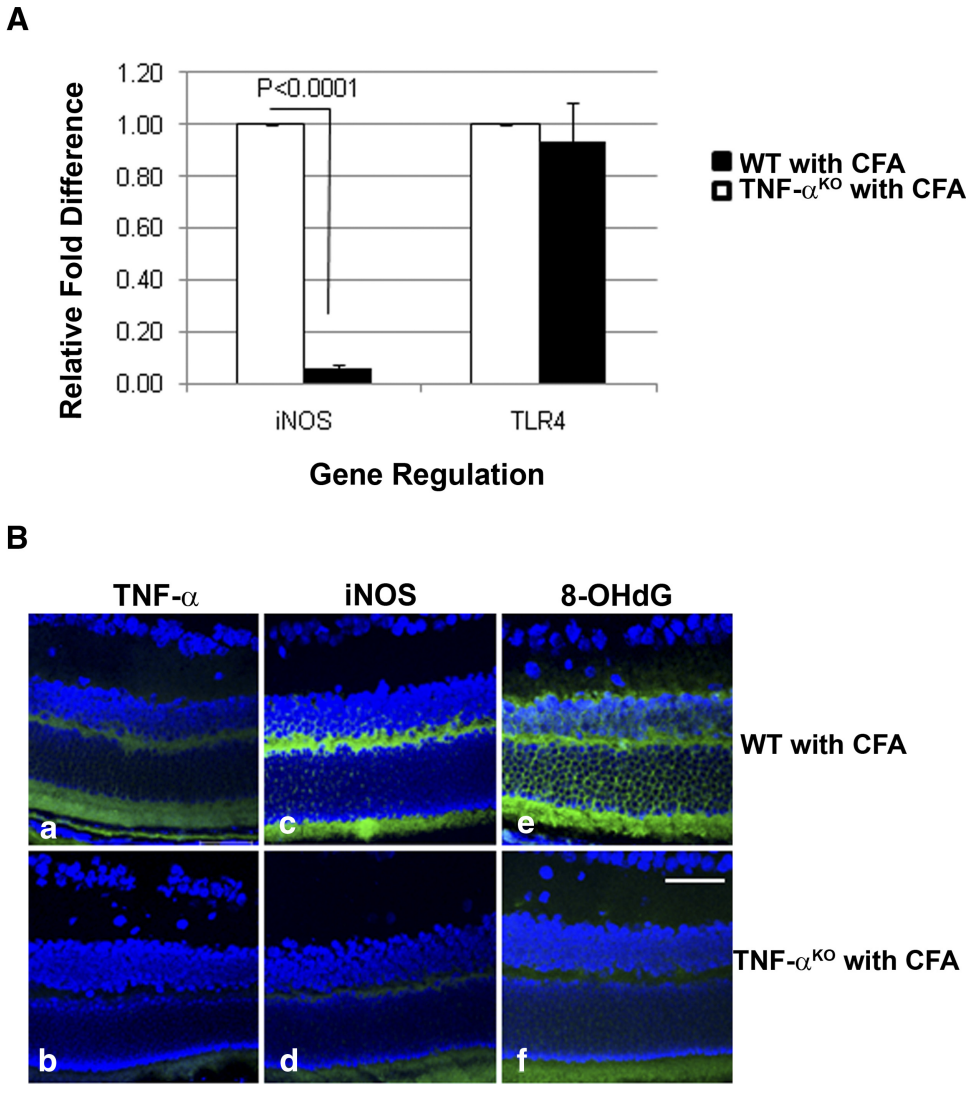

FIGURE 10. Absence of TNF-α–mediated oxidative stress in the retinas of CFA-injected *TNF-*α^{KO} mice. (**A**) Relative fold difference of iNOS and TLR4 gene regulation in the retinas of CFA-injected *TNF-*α^{KO} compared with those of CFA-injected WT. There was no difference in the TLR4 expression between *TNF-*α^{KO} and its WT; however, iNOS was significantly downregulated in the retinas of CFA-injected *TNF-*α^{KO} shown in real-time PCR ($P < 0.0001$; $n = 6$). (**B**) Immunoactivity of *TNF-*α (**a**), iNOS (**c**), and 8-OHdG (**e**) in the retinas of CFA-injected WT were reduced in those of CFA-injected *TNF-*α^{KO} mice (**b**, **d**, **f**). Scale bar, 50 μm.

TNF-α Expression and Localization in the Retina in Innate Immune Response

There was a greater than twofold increase of TNF-α expression in the sera of CFA-injected B10.RIII mice than of IFA-injected mice, as measured by quantitative ELISA (Fig. 9A; $P = 0.02$). Moreover, real-time PCR (Fig. 9B) demonstrated upregulation of the TNF-α mRNA level in the retinas of CFA-injected mice compared with those of IFA-injected mice. Furthermore, Western blot analysis showed the upregulation of TNF-α (Fig. 9C). TNF-α expression was localized in the retina (Fig. 9Db), especially in the IPL, INL, and IS of the photoreceptors, but it was completely absent in the retinas of controls (Fig. 9Da). TNFR1 was localized in the IPL, outer plexiform layer (OPL), and IS of the retinas of the CFA-injected group compared with those of the control group, which showed faint staining in IPL and OPL (Fig. 9Dd vs. 9Dc). In the retinas of CFA-injected mice, TNF-α was colocalized with its receptor, TNFR1, and with 8-OHdG in the IPL, INL, and IS of photoreceptors (Fig. 9Dh vs. 9Dg), indicating that TNF-α may be a major mediator in CFA-mediated oxidative stress in photoreceptors.

The role of TNF-α in CFA-mediated oxidative stress and mtDNA damage was further studied using *TNF-α*^{KO} mice (Fig. 10). There was no alteration of TLR4 expression; however, real-time PCR showed a significant reduction of iNOS ($P < 0.0001$) in retinas of CFA-injected *TNF-α*^{KO} mice (Fig. 10A). Immunostaining of TNF-α (Fig. 10Ba), iNOS (Fig. 10Bc), and 8-OHdG (Fig. 10Be) in the retinas of CFA-injected WT mice was reduced in the retinas of CFA-injected *TNF-α*^{KO} mice (Figs. 10Bb, 10Bd, 10Bf).

Apoptotic Gene Upregulation in CFA-Injected B10.RIII Mice in a Caspase 7-Dependent Manner

To determine whether apoptotic genes were modulated in the retinas of CFA-injected B10.RIII mice, biological triplicates of CFA- or IFA-injected B10.RIII (10 retinas of 5 mice per group were pooled on D5 p.i.) were submitted for PCR array (RT^2 Profiler), which profiles the expression of 84 key genes involved in programmed cell death. In Table 2, 7 of 84 genes were significantly upregulated ($P < 0.005$) in the retinas of CFA-injected B10.RIII mice compared with those of IFA-injected B10.RIII mice. Caspases 1, 4, and 7 showed relative fold increases (1.48-, 3.95-, and 1.37-fold, respectively) in the retinas of the CFA-injected group compared with those of the IFA-injected group. In addition to *NF-κB*, TNF-α–related genes including *Fas, TNFRsf* (TNFR superfamily), and *TRAF1* (TNFR-association factor) were also upregulated (with relative fold differences of 1.2-, 1.53-, 1.2-, and 1.3-fold, respectively).

Caspase 7 is a key mediator for mitochondria-mediated apoptosis along with caspase 3[46]; whereas caspases 1 and 4 are involved in inflammasome formation and activation of inflammatory processes.[47,48] Activated caspase 7 was immunolocalized in the INL and photoreceptor layer of the retinas of CFA-injected B10.RIII mice (Fig. 11Aa), but no caspase 7-positive staining was detected in the noninjected controls (Fig. 11Ab) or the isotype controls (Fig. 11Ac). To further demonstrate whether caspase 7 was a major executioner in the apoptosis processes in the CFA-mediated innate immune response, the retinas of CFA-injected caspase 7^{KO} and its WT were collected for Western blot analysis. CFA-mediated caspase 3 activities were significantly inhibited in CFA-injected caspase 7^{KO} mice (Figs. 11B, 11C) compared with CFA-injected WT mice.

Table 2. Upregulation of Apoptosis-Related Genes in the Retinas of CFA-Injected Mice Compared with Those of IFA-Injected Mice Using PCR Array

Gene	Fold Increase (±SEM)	*P*
Casp1	1.48 (±0.07)	0.0367
Casp4	3.95 (±0.15)	0.0003
Casp7	1.37 (±0.05)	0.0332
Fas	1.53 (±0.10)	0.0240
NF-κB1	1.16 (±0.02)	0.0209
TNFRsf10b	1.22 (±0.04)	0.0225
TRAF1	1.31 (±0.05)	0.0142

Biological triplicates of the CFA- and IFA-injected groups (each sample contained 10 retinas from five mice; day 5 p.i.) were submitted for the PCR array focused on the apoptosis pathway. Among 84 genes involved in the apoptosis pathway, the most significantly modulated genes ($P < 0.05$) are shown. The formula used to calculate the relative gene expression level was $2^{-\Delta\Delta Ct}$ and $\Delta Ct = Ct$ (gene of interest) − Ct (housekeeping gene). Fold change of the gene was calculated by test/control sample. Casp, caspase; Fas, TNF receptor superfamily; NF-κB1, nuclear factor of kappa light polypeptide gene enhancer; TNFRsf, TNF receptor superfamily; TRAF1, TNF receptor-associated factor 1.

Discussion

In the present study, subcutaneous administration of adjuvant with heat-killed *M. tuberculosis* upregulated the expression of innate immune response-related genes, particularly the expression of TLR4, on the retinal microglia. Furthermore, TLR4-mediated mitochondrial oxidative stress and the resultant mtDNA damage were primarily localized to photoreceptor cells. Such mtDNA damage appears to be due to the generation of TNF-α and iNOS in the photoreceptors. The generated iNOS is known to cause mitochondrial oxidative stress and mtDNA damage.[49] Furthermore, these results suggest that prolonged or cumulative TLR activation may lead to severe retinal damage. Although this study is centered on specific TLR activation resulting in early mtDNA damage in photoreceptors, the results support a novel observation that TLR4 activation and its signal transduction can cause oxidative stress-mediated retinal mitochondrial DNA damage before the initiation of adaptive immune-mediated tissue damage.

B10.RIII mice used in the experiments are known to be highly susceptible for the induction of EAU and other autoimmune diseases.[50,51] In addition, various knockout animals were used along with their WT (C57BL/6J), and the effect of CFA-mediated activation of innate immune response was similar to that seen in the B10.RIII mice.

It is intriguing that we found the genome of bacterial DNA in the retinas after subcutaneous injection of heat-killed mycobacteria in the adjuvant using the qPCR, especially after intracardiac perfusion with saline-containing heparin. The finding of such DNA in the mouse brain, liver, and spleen suggests that the route of bacterial dissemination is through circulation. However, it is not clear from our experimental results whether the bacterial DNA is within the retinal microglia. Recent reports[52] suggest that the blood-brain barrier is altered after such subcutaneous injection of dead organisms administered in conjunction with complete Freund's adjuvant. Furthermore, macrophages are reported to phagocytose mycobacterium to disseminate the organism to various organs.[53] Thus, it is plausible that subcutaneously injected heat-killed bacteria are phagocytosed by infiltrating macrophages and that they can subsequently travel to the liver, spleen, retina, and other organs. The blood-ocular barrier could be altered by CFA injection, thus facilitating bacterial DNA entry into the retina. Further studies are required in bone marrow chimeric mice to address the dissemination of heat-killed mycobacteria to the retina, brain, liver, and spleen.

Similar TLR4 activation can be obtained by the injection of LPS, but this agent induces the infiltration of B cells and

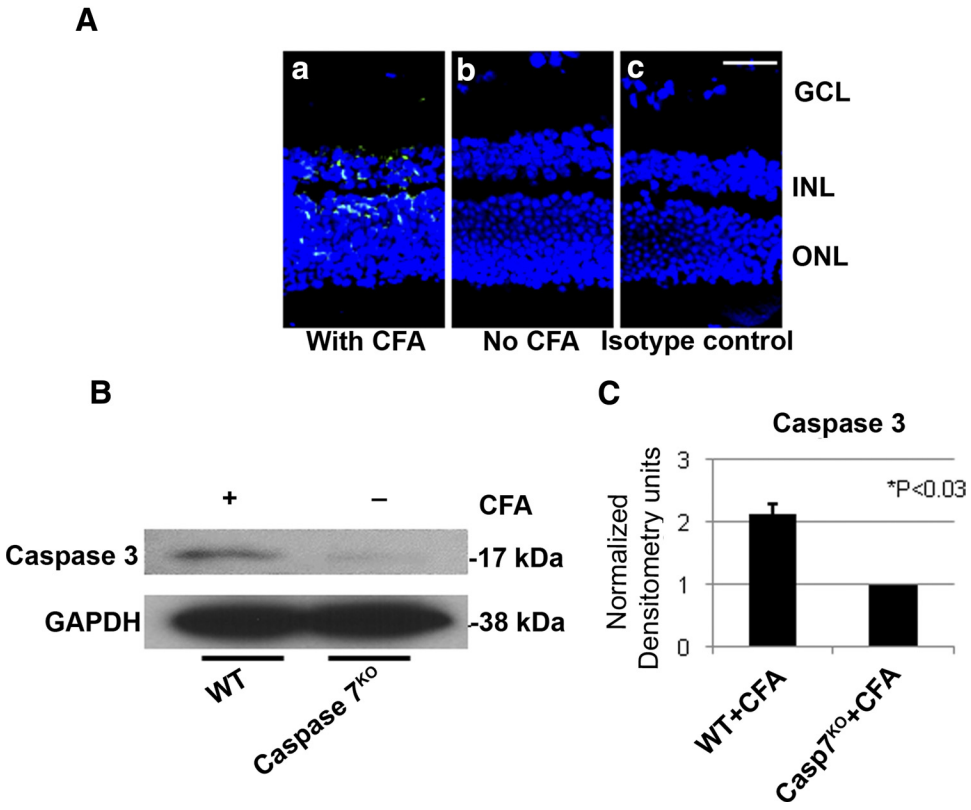

FIGURE 11. Caspase 7-dependent apoptotic activity in innate immune response. (**A**) Caspase 7 was localized in the INL and outer nuclear layer (ONL) of photoreceptor in the CFA-injected B10.RIII mice (**a**, *green*), whereas such staining was absent in the noninjected (**b**) and isotype (**c**) controls. Scale bar, 50 μm. (**B**) Caspase 7^{KO} and its WT control were injected with CFA, and the retinas were collected on day 5 p.i for Western blot analysis. CFA-mediated caspase 3 activity was significantly reduced in the retinas of CFA-injected caspase 7^{KO} mice. Cell lysates (40 μg) were separated by SDS-PAGE on 15% reduced gel; rabbit anti-caspase 3 or mouse anti-GAPDH was used as a primary antibody, followed by HRP-conjugated anti-rabbit or mouse antibody. (**C**) These bands shown in Western blot analysis of biological triplicates (**B**) were measured and showed that the activity of caspase 3 was inhibited significantly ($^*P < 0.03$).

neutrophils within a few hours after foot pad injection.[54] In addition, LPS can promptly stimulate T cells.[55] Hence, the induction of TLR expression in the retina by CFA injection at a remote site (away from the eye) offers an ideal model with which to dissect TLR functions in the absence of leukocyte infiltration and a model for in vivo dissection of the early innate immune response of ocular inflammation involved in mitochondrial oxidative damage in the retina.

Perivascular microglia are crucial cellular components of the innate immune system in the CNS.[56,57] Such microglia in the retina are bone marrow derived,[58] and in CNS they may constitutively express low levels of TLR.[56] In our studies, TLR4 was upregulated and was immunohistochemically localized on the microglia. The microglia also expressed MHC class II molecules, indicating the microglial cells were in an activated state. Moreover, such oxidative stress was not restricted to the microglial cells expressing TLR; it was also seen in the adjacent INL and photoreceptor cells. We showed that TNF-α may mediate photoreceptor oxidative stress/mtDNA damage in a paracrine manner; but Santos et al.[59] demonstrated the migration and accumulation of activated microglia to the insult site in photoreceptor degeneration, suggesting the possibility of direct communication by microglia in such oxidative stress in the photoreceptor. The mycobacteria in CFA are assumed to be recognized by TLRs on various immunocompetent cells and to play a role in the activation of the innate immune compartment, especially the Th1-type ongoing immune response.[21]

With the exception of TLR3, TLR signals primarily through the MyD88-dependent pathway. In the in vivo biological system using *MyD88*^{KO} animals, we addressed the significance of the MyD88 interaction with TLR in the signaling pathway and its role in oxidative stress. There was no oxidative DNA damage in the retinas of *MyD88*^{KO} mice after CFA injection, indicating the MyD88-dependent pathway is the major pathway in the induction of oxidative stress. However, the contribution of other TLR4 and TLR3 adapters—the TIR-domain-containing adapter-inducing interferon-β (TRIF/TRAM)-mediated pathway—will be determined in the MyD88 or TRIF knockout mouse, or both.[60]

This study provides novel observations of TLR4-mediated photoreceptor mitochondrial oxidative stress and selective mtDNA damage in the innate immune response. Understanding the molecular mechanism of photoreceptor damage caused by the TLR4/MyD88/TNF-α/iNOS cascade in the retina could provide a unique model with which to study the damaging effects of TLR expression and to develop novel therapeutic strategies for rescuing photoreceptors and other neuronal cells of the retina, CNS, and other tissues exposed to the axis of TLR-oxidative stress.

Acknowledgments

The authors thank Deming Sun for MyD88^{KO} mice and for helpful discussions.

References

1. Waldner H. The role of innate immune responses in autoimmune disease development. *Autoimmun Rev.* 2009;8:400–404.
2. Takeda K, Kaisho T, Akira S. Toll-like receptors. *Annu Rev Immunol.* 2003;21:335–376.
3. Spivak N, Bogdanova IM, Martirosova NI, Malaitsev VV. The role of Toll-like receptors in regulation of immune responses in norm and pathology. *Fiziol Zh.* 2008;54:87–99.
4. Rifkin IR, Leadbetter EA, Busconi L, Viglianti G, Marshak-Rothstein A. Toll-like receptors, endogenous ligands, and systemic autoimmune disease. *Immunol Rev.* 2005;204:27–42.
5. Olson JK, Miller SD. Microglia initiate central nervous system innate and adaptive immune responses through multiple TLRs. *J Immunol.* 2004;173:3916–3924.
6. Medzhitov R. Toll-like receptors and innate immunity. *Nat Rev Immunol.* 2001;1:135–145.

7. Yamamoto M, Takeda K, Akira S. TIR domain-containing adaptors define the specificity of TLR signaling. *Mol Immunol.* 2004;40: 861–868.
8. O'Neill LA, Fitzgerald KA, Bowie AG. The Toll-IL-1 receptor adaptor family grows to five members. *Trends Immunol.* 2003;24:286–290.
9. Vogel SN, Fitzgerald KA, Fenton MJ. TLRs: differential adapter utilization by toll-like receptors mediates TLR-specific patterns of gene expression. *Mol Interv.* 2003;3:466–477.
10. Lee SJ, Lee S. Toll-like receptors and inflammation in the CNS. *Curr Drug Targets Inflamm Allergy.* 2002;1:181–191.
11. Sakon S, Xue X, Takekawa M, et al. NF-kappaB inhibits TNF-induced accumulation of ROS that mediate prolonged MAPK activation and necrotic cell death. *EMBO J.* 2003;22:3898–3909.
12. Ha T, Li Y, Hua F, et al. Reduced cardiac hypertrophy in toll-like receptor 4-deficient mice following pressure overload. *Cardiovasc Res.* 2005;68:224–234.
13. Hua F, Ma J, Ha T, et al. Activation of Toll-like receptor 4 signaling contributes to hippocampal neuronal death following global cerebral ischemia/reperfusion. *J Neuroimmunol.* 2007;190:101–111.
14. Kim BS, Lim SW, Li C, et al. Ischemia-reperfusion injury activates innate immunity in rat kidneys. *Transplantation.* 2005;79:1370–1377.
15. Sacre SM, Andreakos E, Kiriakidis S, et al. The Toll-like receptor adaptor proteins MyD88 and Mal/TIRAP contribute to the inflammatory and destructive processes in a human model of rheumatoid arthritis. *Am J Pathol.* 2007;170:518–525.
16. Schroder NW, Arditi M. The role of innate immunity in the pathogenesis of asthma: evidence for the involvement of Toll-like receptor signaling. *J Endotoxin Res.* 2007;13:305–312.
17. Shimamoto A, Pohlman TH, Shomura S, et al. Toll-like receptor 4 mediates lung ischemia-reperfusion injury. *Ann Thorac Surg.* 2006;82:2017–2023.
18. Zhai Y, Shen XD, O'Connell R, et al. Cutting edge: TLR4 activation mediates liver ischemia/reperfusion inflammatory response via IFN regulatory factor 3-dependent MyD88-independent pathway. *J Immunol.* 2004;173:7115–7119.
19. Tobias PS, Curtiss LK. Toll-like receptors in atherosclerosis. *Biochem Soc Trans.* 2007;35:1453–1455.
20. Edwards AO, Chen D, Fridley BL, et al. Toll-like receptor polymorphisms and age-related macular degeneration. *Invest Ophthalmol Vis Sci.* 2008;49:1652–1659.
21. Billiau A, Matthys P. Modes of action of Freund's adjuvants in experimental models of autoimmune diseases. *J Leukoc Biol.* 2001;70:849–860.
22. Petty RE, Johnston W, McCormick AQ, et al. Uveitis and arthritis induced by adjuvant: clinical, immunologic and histologic characteristics. *J Rheumatol.* 1989;16:499–505.
23. Chillingworth NL, Donaldson LF. Characterisation of a Freund's complete adjuvant-induced model of chronic arthritis in mice. *J Neurosci Methods.* 2003;128:45–52.
24. Bulut Y, Faure E, Thomas L, Equils O, Arditi M. Cooperation of Toll-like receptor 2 and 6 for cellular activation by soluble tuberculosis factor and *Borrelia burgdorferi* outer surface protein A lipoprotein: role of Toll-interacting protein and IL-1 receptor signaling molecules in Toll-like receptor 2 signaling. *J Immunol.* 2001;167:987–994.
25. Quesniaux V, Fremond C, Jacobs M, et al. Toll-like receptor pathways in the immune responses to mycobacteria. *Microbes Infect.* 2004;6:946–959.
26. Suliman HB, Welty-Wolf KE, Carraway MS, et al. Toll-like receptor 4 mediates mitochondrial DNA damage and biogenic responses after heat-inactivated E. coli. *FASEB J.* 2005;19:1531–1533.
27. Liang FQ, Godley BF. Oxidative stress-induced mitochondrial DNA damage in human retinal pigment epithelial cells: a possible mechanism for RPE aging and age-related macular degeneration. *Exp Eye Res.* 2003;76:397–403.
28. Qi X, Lewin AS, Sun L, Hauswirth WW, Guy J. Suppression of mitochondrial oxidative stress provides long-term neuroprotection in experimental optic neuritis. *Invest Ophthalmol Vis Sci.* 2007; 48:681–691.
29. Yakes FM, Van Houten B. Mitochondrial DNA damage is more extensive and persists longer than nuclear DNA damage in human cells following oxidative stress. *Proc Natl Acad Sci U S A.* 1997; 94:514–519.
30. Van Houten B, Woshner V, Santos JH. Role of mitochondrial DNA in toxic responses to oxidative stress. *DNA Repair (Amst).* 2006; 5:145–152.
31. Khurana RN, Parikh JG, Saraswathy S, Wu GS, Rao NA. Mitochondrial oxidative DNA damage in experimental autoimmune uveitis. *Invest Ophthalmol Vis Sci.* 2008;49:3299–3304.
32. Saraswathy S, Rao NA. Photoreceptor mitochondrial oxidative stress in experimental autoimmune uveitis. *Ophthalmic Res.* 2008; 40:160–164.
33. Saraswathy S, Rao NA. Mitochondrial proteomics in experimental autoimmune uveitis oxidative stress. *Invest Ophthalmol Vis Sci.* 2009;50:5559–5566.
34. Livak KJ, Schmittgen TD. Analysis of relative gene expression data using real-time quantitative PCR and the $2\Delta\Delta C_T$ method. *Methods.* 2001;25:402–408.
35. Broccolo F, Scarpellini P, Locatelli G, et al. Rapid diagnosis of mycobacterial infections and quantitation of *Mycobacterium tuberculosis* load by two real-time calibrated PCR assays. *J Clin Microbiol.* 2003;41:4565–4572.
36. Santos JH, Meyer JN, Mandavilli BS, Van Houten B. Quantitative PCR-based measurement of nuclear and mitochondrial DNA damage and repair in mammalian cells. *Methods Mol Biol.* 2006;314:183–199.
37. Wang AL, Lukas TJ, Yuan M, Neufeld AH. Increased mitochondrial DNA damage and down-regulation of DNA repair enzymes in aged rodent retinal pigment epithelium and choroid. *Mol Vis.* 2008;14: 644–651.
38. Rival C, Theas MS, Guazzone VA, Lustig L. Interleukin-6 and IL-6 receptor cell expression in testis of rats with autoimmune orchitis. *J Reprod Immunol.* 2006;70:43–58.
39. Triantafilou M, Triantafilou K. Lipopolysaccharide recognition: CD14, TLRs and the LPS-activation cluster. *Trends Immunol.* 2002; 23:301–304.
40. Wang JY, Lin CG, Hsiao YH, Liou YH, Wu LS. Single nucleotide polymorphisms and haplotype of MD-1 gene associated with high serum IgE phenotype with mite-sensitive allergy in Taiwanese children. *Int J Immunogenet.* 2007;34:407–412.
41. Williams CS, Mann M, DuBois RN. The role of cyclooxygenases in inflammation, cancer, and development. *Oncogene.* 1999;18: 7908–7916.
42. Xu H, Chen M, Mayer EJ, Forrester JV, Dick AD. Turnover of resident retinal microglia in the normal adult mouse. *Glia.* 2007; 55:1189–1198.
43. Feng CG, Kaviratne M, Rothfuchs AG, et al. NK cell-derived IFN-gamma differentially regulates innate resistance and neutrophil response in T cell-deficient hosts infected with Mycobacterium tuberculosis. *J Immunol.* 2006;177:7086–7093.
44. Kim KD, Zhao J, Auh S, et al. Adaptive immune cells temper initial innate responses. *Nat Med.* 2007;13:1248–1252.
45. Smoak KA, Aloor JJ, Madenspacher J, et al. Myeloid differentiation primary response protein 88 couples reverse cholesterol transport to inflammation. *Cell Metab.* 11:493–502.
46. Lakhani SA, Masud A, Kuida K, et al. Caspases 3 and 7: key mediators of mitochondrial events of apoptosis. *Science.* 2006;311: 847–851.
47. Mariathasan S, Newton K, Monack DM, et al. Differential activation of the inflammasome by caspase-1 adaptors ASC and Ipaf. *Nature.* 2004; 430:213–218.
48. Martinon F, Tschopp J. Inflammatory caspases and inflammasomes: master switches of inflammation. *Cell Death Differ.* 2007;14:10–22.
49. Druzhyna NM, Musiyenko SI, Wilson GL, LeDoux SP. Cytokines induce nitric oxide-mediated mtDNA damage and apoptosis in oligodendrocytes: protective role of targeting 8-oxoguanine glycosylase to mitochondria. *J Biol Chem.* 2005;280:21673–21679.
50. Myers LK, Miyahara H, Terato K, et al. Collagen-induced arthritis in B10.RIII mice (H-2r): identification of an arthritogenic T-cell determinant. *Immunology.* 1995;84:509–513.
51. Silver PB, Chan CC, Wiggert B, Caspi RR. The requirement for pertussis to induce EAU is strain-dependent: B10.RIII, but not B10.A mice, develop EAU and Th1 responses to IRBP without pertussis treatment. *Invest Ophthalmol Vis Sci.* 1999;40:2898–2905.

52. Rabchevsky AG, Degos JD, Dreyfus PA. Peripheral injections of Freund's adjuvant in mice provoke leakage of serum proteins through the blood-brain barrier without inducing reactive gliosis. *Brain Res.* 1999;832:84–96.
53. Davis JM, Ramakrishnan L. The role of the granuloma in expansion and dissemination of early tuberculous infection. *Cell.* 2009;136:37–49.
54. Tough DF, Sun S, Sprent J. T cell stimulation in vivo by lipopolysaccharide (LPS). *J Exp Med.* 1997;185:2089–2094.
55. Akira S, Uematsu S, Takeuchi O. Pathogen recognition and innate immunity. *Cell.* 2006;124:783–801.
56. Lehnardt S, Massillon L, Follett P, et al. Activation of innate immunity in the CNS triggers neurodegeneration through a Toll-like receptor 4-dependent pathway. *Proc Natl Acad Sci U S A.* 2003;100:8514–8519.
57. Lehnardt S, Schott E, Trimbuch T, et al. A vicious cycle involving release of heat shock protein 60 from injured cells and activation of toll-like receptor 4 mediates neurodegeneration in the CNS. *J Neurosci.* 2008;28:2320–2331.
58. Albini TA, Wang RC, Reiser B, et al. Microglial stability and repopulation in the retina. *Br J Ophthalmol.* 2005;89:901–903.
59. Santos AM, Martin-Oliva D, Ferrer-Martin RM, et al. Microglial response to light-induced photoreceptor degeneration in the mouse retina. *J Comp Neurol.* 2010;518:477–492.
60. Kawai T, Akira S. TLR signaling. *Semin Immunol.* 2007;19:24–32.